

- Supporting Information -

Chemical Interaction, Space-charge Layer and Molecule Charging Energy for Metal Oxide/Organic interfaces

José I. Martínez,^{a,} Fernando Flores,^b José Ortega,^b Sylvie Rangan,^c*

Charles Ruggieri,^c and Robert A. Bartynski^c

^a Dept. Surfaces, Coatings and Molecular Astrophysics,

Institute of Material Science of Madrid (ICMM-CSIC), ES-28049 Madrid (Spain)

^b Dept. Condensed Matter Theoretical Physics and Condensed Matter Physics Center (IFIMAC),

Autonomous University of Madrid, ES-28049 Madrid (Spain)

^c Dept. Physics and Astronomy, and Laboratory for Surface Modification,

Rutgers, The State University of New Jersey, Piscataway, NJ 08854-8019 (USA)

*E-mail: joseignacio.martinez@icmm.csic.es

1. Experimental Methods

1.1 Spectroscopic methods

X-ray and ultraviolet photoemission spectroscopies (XPS and UPS), as well as inverse photoemission spectroscopy (IPS) measurements, were performed in a single UHV experimental system described elsewhere.^{S1} Core levels were probed using X-ray photoemission spectroscopy

excited by non-monochromatized Al K α radiation, and the valence band electronic states were examined using He II (40.8 eV) excited ultraviolet photoemission spectroscopy. In both cases, electron energy distributions were measured using a cylindrical mirror analyzer. The conduction band spectra were obtained from IPS performed using a grating spectrometer with a primary electron energy of 20.3 eV. The overall energy resolution for the UPS and IPS spectra is estimated to be better than 0.3 and 0.6 eV, respectively. The energy scales of the UPS and IPS spectra were calibrated using the measured position of the Fermi level of a gold sample in contact with the oxide sample. The secondary electron cutoff has been measured on a biased sample using He I (21.1 eV) to determine the electron affinity, given by $EA = hv - W - E_{\text{gap}}$, where hv is the photon source energy, W the total width of the spectrum, and E_{gap} is the experimentally measured gap of the oxide surfaces or the molecular gap.

1.2 Sample preparation

The rutile TiO₂(110) sample was a commercially produced single-crystal from MTI corporation, cut to within 0.5° of the (110) plane. The sample was degassed and prepared in an ultrahigh vacuum using several cycles of 1 keV Ar⁺ ion sputtering (while maintaining a maximum sample current of 2 μ A) and annealing in UHV at 900K. The cleanliness of the surfaces was checked using XPS, and UPS. TCNQ (Aldrich, 98% purity) was then sublimated in the same chamber, from a thoroughly degassed Knudsen cell held at 390K.

1.3 Surface characterization

Figure S1 shows large scale survey scans before and after saturation with TCNQ at *RT*. These data indicate that, as expected, after a monolayer saturation, only C 1s and N 1s core levels are added to the initial Ti 2p and O 1s core levels belonging to the surface. The molecular

coverage can be evaluated by comparing the relative ratio of C 1s and Ti 2p core levels to no more than a monolayer.

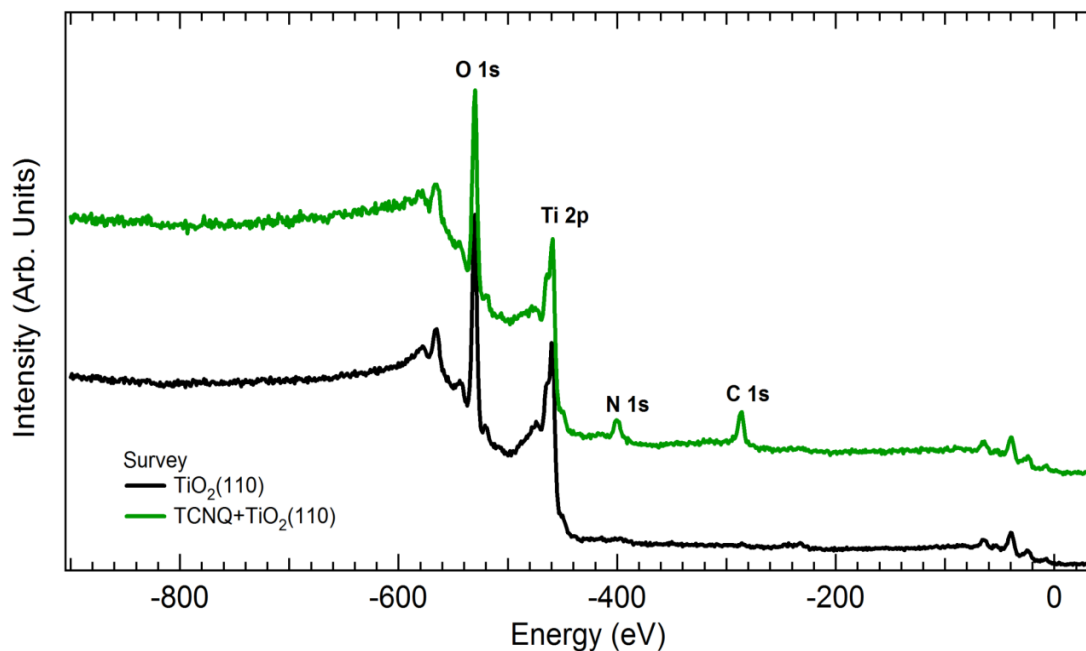


Figure S1. Survey scans of the $\text{TiO}_2(110)$ surface before and after saturation with TCNQ at room temperature. The main core levels are labeled and used for coverage determination.

Figure S2 shows the valence and conduction spectra for a TCNQ multilayer on Cu at 230K as well as the Density of States (DOS) for the gas phase molecule calculated^{S2} using the B3LYP exchange-correlation functional and a 6-31G basis set, with a scissor operator applied to align to experimental features. The DOS was calculated by performing a sum of the individual electronic states convoluted with a 1 eV full width half maximum gaussian function. The energy diagram, Figure S2(b), can be expected to be similar for other multilayer cases. However, for a TCNQ monolayer on TiO_2 the energy gap is reduced to 3.6 eV; assuming this narrowing of the gap to be symmetric around the mid-gap, we find the LUMO level at 4.4 eV from vacuum. Notice that this energy has a resolution of around 0.6 eV.

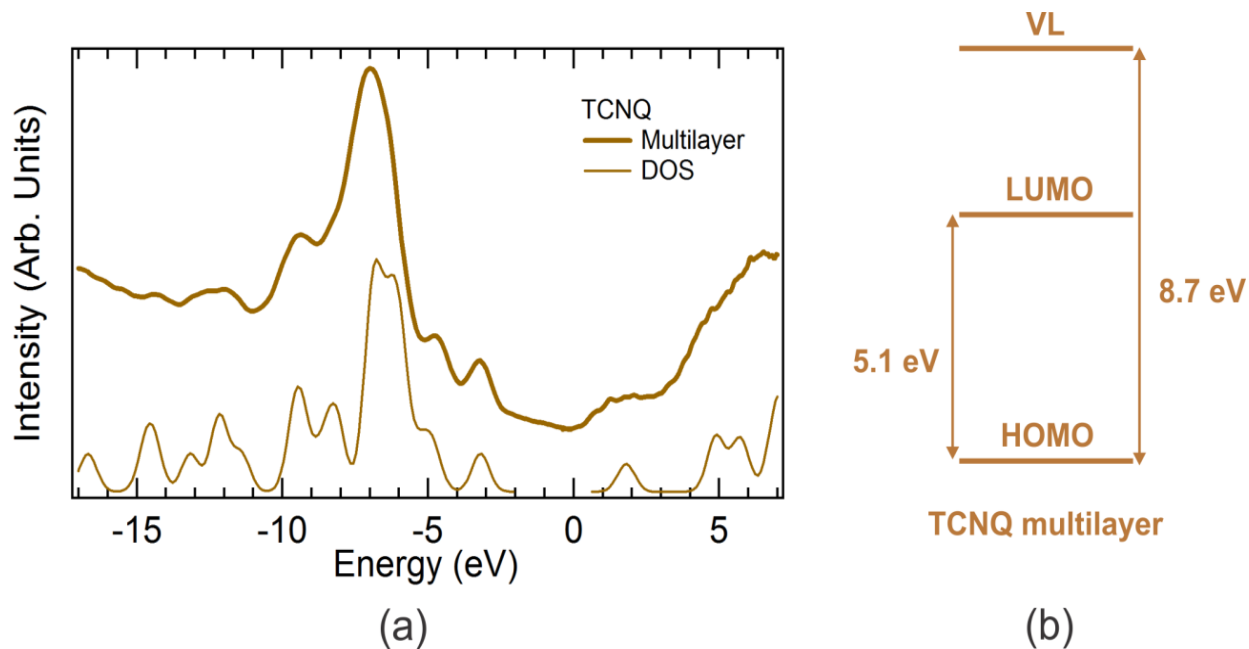


Figure S2. (a) Valence and conduction band spectra measured using UPS and IPS respectively, of a TCNQ multilayer on Cu at 230K compared to a calculated TCNQ gas phase DOS, and (b) corresponding energy diagram. The zero of energy is chosen as the position of the Fermi level.

2. Theoretical Methods

In our calculations we have used the efficient local-orbital DFT code FIREBALL.^{S3–S6} This technique is based on a local-orbital formulation of DFT in which self-consistency is implemented on the orbital occupation numbers;^{S6, S7} these orbital occupation numbers have been obtained using the orthonormal Löwdin orbitals.^{S3–S6} We have used a basis set of optimized *spd* numerical atomic orbitals (NAOs)^{S8} for C, N and Ti, *ss*pp** for O and *s* for H, with cut-off radii (in a.u.): $s = 4.0$, $p = 4.5$ and $d = 5.4$ (C); $s = 3.6$, $p = 4.1$ and $d = 5.2$ (N); $s = 6.2$, $p = 6.7$, $d = 5.7$ (Ti); $s = s^* = 3.4$, $p = p^* = 3.8$ (O); and $s = 4.1$ (H). This is the same basis set as used in other previous works involving TCNQ interfaces. In our calculations we have used the Local Density Approximation (LDA) functional^{S5} and the ion-electron interaction as modelled by means of norm-conserving scalar-relativistic pseudo-potentials.^{S9}

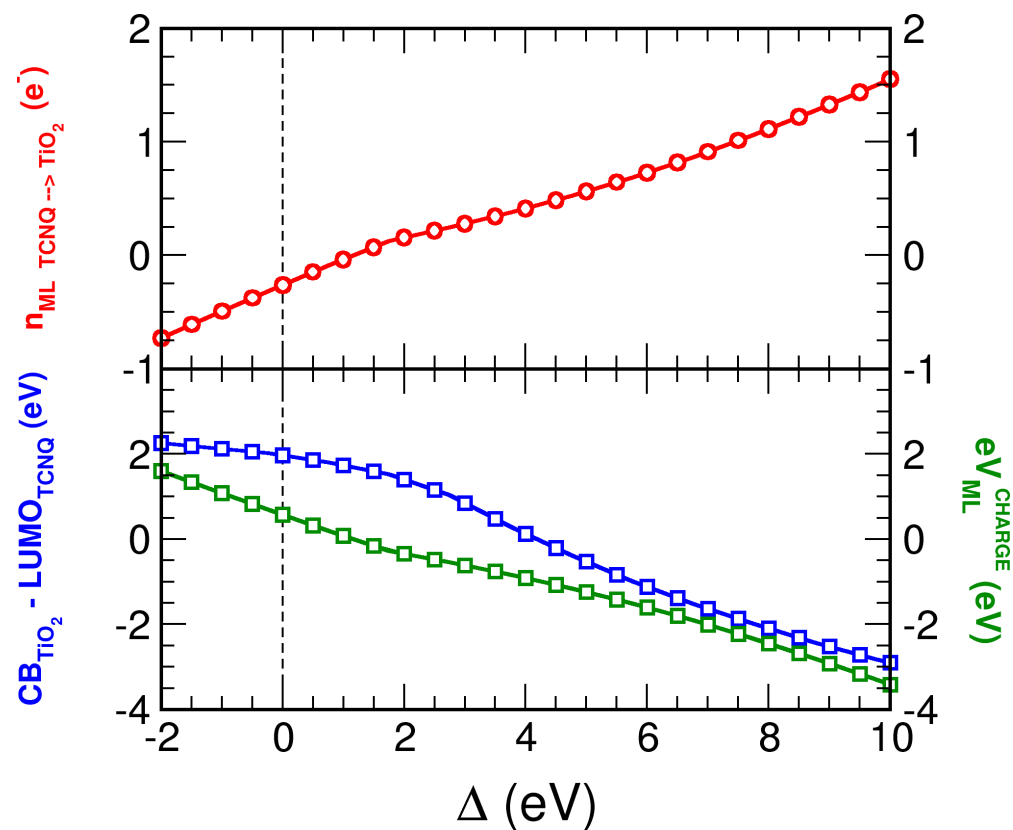


Figure S3. Charge transfer, n_{ML} (in e^- units), E_C -LUMO (in eV) and eV_{ML}^{charge} (in eV) at 0K for a TCNQ monolayer.

Figure S3 shows our calculations for the TCNQ / oxide charge transfer, in electron units, and $(E_C - LUMO)$ as a function of a fictitious shift, Δ , applied to the TCNQ levels. These calculations are performed at 0K using FIREBALL, as well as the operator defined in the text by Equation (1). The effect of $1e^-$ transfer to the LUMO level is simulated by taking $\Delta = 2.2$ eV.

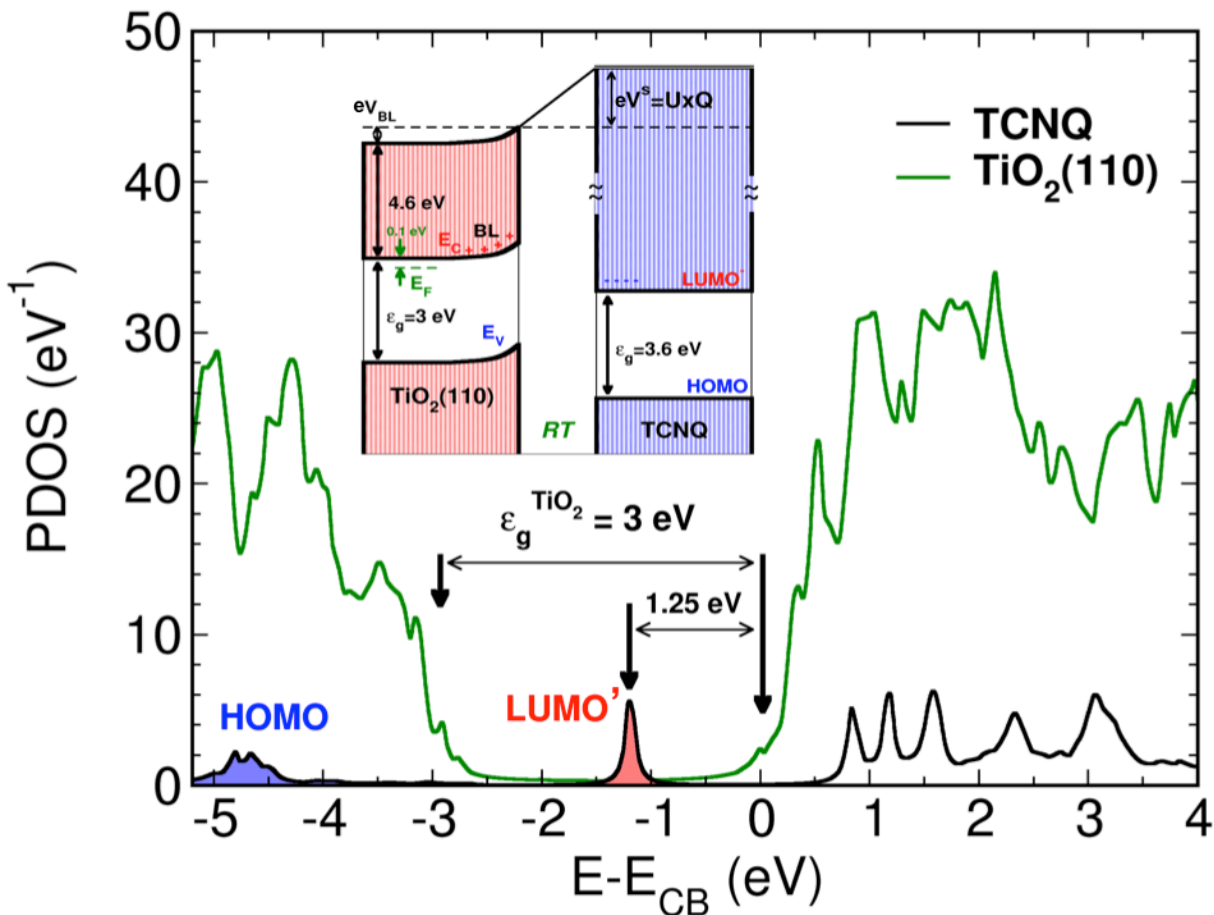


Figure S4. Projected DOS onto the TCNQ molecule and the TiO_2 first layer, for the TCNQ / TiO_2 interface (1 ML) at RT. The inset shows the space charge potential and the molecule charging energy induced by the electron transfer to the LUMO level.

Figure S4 shows the projected Density of States onto TCNQ and a layer of TiO_2 after introducing the Δ_0 -shift in the molecular levels. At RT a space charge is created in the oxide due to the electron transfer to the LUMO level; this charge transfer is simulated in our calculations introducing that Δ_0 -shift in the molecular levels.

3. Details of the Pristine TiO₂(110) Band-edges

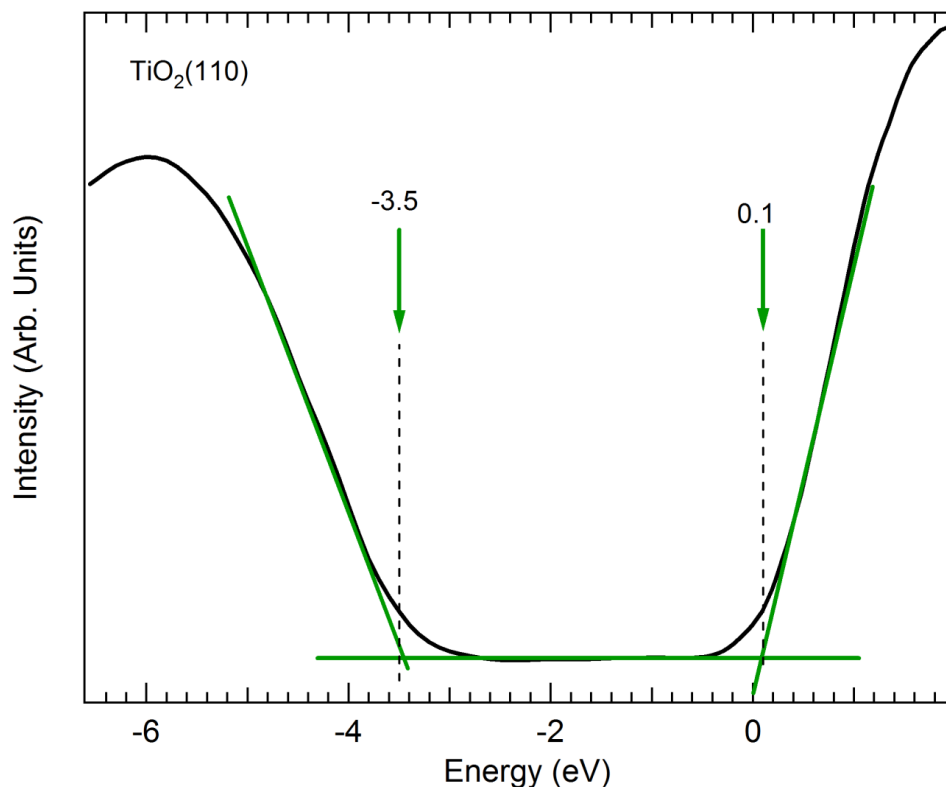


Figure S5. Details of the pristine TiO₂(110) band edges. The edges are determined as the intersection of the linearly fitted band edges with the flat spectral background. The VB edge is estimated at -3.5 eV and the CB edge at 0.1 eV.

References

- (S1) E. Bersch, S. Rangan, R. A. Bartynski, E. Garfunkel, E. Vescovo, *Phys. Rev. B* **2008**, 78, 085114.
- (S2) M. W. Schmidt, K. K. Baldrige, J. A. Boatz, S. T. Elbert, M. S. Gordon, J. H. Jensen, S. Koseki, N. Matsunaga, K. A. Nguyen, S. J. Su, T. L. Windus, M. Dupuis, J. A. Montgomery, *J. Comput. Chem.* **1993**, 14, 1347.
- (S3) J. P. Lewis, P. Jelínek, J. Ortega, A. A. Demkov, D. G. Trabada, B. Haycock, H. Wang, G. Adams, J. K. Tomfohr, E. Abad, H. Wang, D. A. Drabold, *Phys. Stat. Sol. B* **2011**, 248, 1989.

- (S4) J. P. Lewis, K. R. Glaesemann, G. A. Both, J. Fritsch, A. A. Demkov, J. Ortega, O. F. Sankey, *Phys. Rev. B* **2001**, *64*, 195103.
- (S5) P. Jelínek, H. Wang, J. P. Lewis, O. F. Sankey, J. Ortega, *Phys. Rev. B* **2005**, *71*, 235101.
- (S6) A. A. Demkov, J. Ortega, O. F. Sankey, M. P. Grumbach, *Phys. Rev. B* **1995**, *52*, 1618.
- (S7) F. J. García-Vidal, J. Merino, R. Pérez, R. Rincón, J. Ortega, F. Flores, *Phys. Rev. B* **1994**, *50*, 10537.
- (S8) M. A. Basanta, Y. J. Dappe, P. Jelínek, J. Ortega, *Comput. Mater. Sci.* **2007**, *39*, 759.
- (S9) M. Fuchs, M. Scheffler, *Comput. Phys. Commun.* **1999**, *119*, 67.